Development and validation of an immunohistochemistry procedure for the detection of a neurotropic bovine astrovirus

Céline L. Boujon [a], Senija Selimovic-Hamza [a,b], Ilias Bouzalas [a], Torsten Seuberlich [a,*]

[a] NeuroCenter, Division of Neurological Sciences, Vetsuisse Faculty, University of Bern, Bremgartenstrasse 109A, CH-3012, Bern, Switzerland
[b] Graduate School for Cellular and Biomedical Sciences, University of Bern, Freiestrasse 1, CH-3012, Bern, Switzerland

ABSTRACT

Members of the *Astroviridae* family are best known to cause diarrhea in different mammalian species. Lately, some strains have been associated with encephalitis in humans, minks and cattle. In this study, we developed an immunohistochemistry (IHC) procedure for the detection of a neurotropic bovine astrovirus (BoAstV-CH13/NeuroS1), which is associated with non-suppurative encephalitis in cattle. We expressed five recombinant antigens corresponding to different putative viral proteins of BoAstV-CH13/NeuroS1. Antigens were then used for the production of hyperimmune sera in rabbits. Out of the five hyperimmune sera, the one directed against the conserved N-terminus of the viral capsid protein, termed ORF2-con, clearly surpassed the others in the detection of viral antigens in IHC in terms of strong signal intensity and low background staining. The accuracy of the ORF2-con IHC protocol was then evaluated using different sets of brain tissue samples: 30 samples from 9 animals with confirmed BoAstV-CH13/NeuroS1 infection, 30 samples from 8 animals with non-suppurative encephalitis of another etiology and 30 samples from apparently healthy slaughtered animals. The IHC was positive only with tissue samples from animals with a known positive BoAstV-CH13/NeuroS1 status, but not with those from negative ones, indicating a good diagnostic sensitivity and specificity of the assay. The ORF2-con IHC procedure is therefore an adequate tool for the detection of BoAstV-CH13/NeuroS1 infections in cattle.

1. Introduction

Astroviridae are small viruses with a star-like appearance in electron microscopy (Caul and Appleton, 1982). Members of this family are non-enveloped viruses and have a positive sense, single-stranded RNA genome of 6.2 to 7.8 kb. The first astrovirus to be discovered was isolated in 1975 from stool samples of children suffering from diarrhea (Appleton and Higgins, 1975). Since then, astroviruses have been found in the feces of many species but, apart from humans (especially children), in which they are recognized as a leading cause of diarrhea, their association with enteric dis-

ease has not been found to be consistent. In cattle, for example, animals experimentally infected with a *bovine astrovirus* (BoAstV) did not develop clinical disease (Woode and Bridger, 1978; Woode et al., 1984), and excretion of the virus was found to be variable (Alfred et al., 2015; Tse et al., 2011). In recent years, novel astroviruses have been found in several cases of encephalitis in different species: humans (Brown et al., 2015; Cordey et al., 2016; Fremond et al., 2015; Naccache et al., 2015; Quan et al., 2010; Sato et al., 2016; Saylor et al., 2015; Thakur and Venkatesan, 2015; Wunderli et al., 2011), minks (Blomstrom et al., 2010) and cattle (Bouzalas et al., 2014; Li et al., 2013; Schlottau et al., 2016; Seuberlich et al., 2016). In cattle, it seems that two different types of neurotropic astroviruses occur: BoAstV-CH13/NeuroS1 (Bouzalas et al., 2016; Li et al., 2013) and BoAstV-CH15 (Seuberlich et al., 2016), the latter being very similar to another bovine neurotropic virus that has been found in Germany lately (Schlottau et al., 2016). Both have been found in cases of so-called European sporadic bovine encephalitis (ESBE), a disease characterized histologically by a non-suppurative inflammation pattern (Fankhauser, 1961) but with a heterogeneous, in some cases unknown etiology. So far, BoAstV-CH15 was found only in two animals, but BoAstV-CH13/NeuroS1 infections seem to be

more frequent, as the virus was detected in brain tissues of around one quarter of animals with ESBE.

Different methods have been used to detect BoAstV-CH13/NeuroS1: next-generation sequencing (NGS), reverse transcription PCR (RT-PCR), and in situ hybridization (ISH) (Bouzalas et al., 2014; Li et al., 2013). NGS has the advantage of providing details about the sequences found, but is not adequate for testing large number of samples. RT-PCR is a quick and handy method. However, both techniques do not allow a reliable *in situ* detection of the virus. Procedures that are suitable for use with formalin-fixed, paraffin embedded (FFPE) material, which is the most common type of tissue sample in pathology, facilitate pathogen identification on archived material and retrospective prevalence studies. Whereas ISH is a well suited and sensitive approach to this end, it is technically demanding and time-consuming. Therefore, our aim was to develop a robust, time-efficient and cost-effective method for the diagnosis and further characterization of BoAstV-CH13/NeuroS1 in FFPE tissues. Consequently, immunohistochemistry (IHC) was the method of choice. For this purpose, we expressed five different recombinant viral antigens, which were then used for the production of hyperimmune sera in rabbits. After optimization of the IHC protocol, the method was tested on different sets of samples in order to evaluate its accuracy. The hyperimmune serum raised against the conserved N-terminus of the viral capsid protein provided sensitive and specific results in IHC, comparable to those obtained with ISH.

2. Materials and methods

2.1. Design of the recombinant viral antigens

Initially, we attempted to produce three antigens corresponding to the full-length primary translation products of each ORF (ORF1a, ORF1b, ORF2). While we were able to amplify the entire coding region of ORF1b by RT-PCR, this was not possible for ORF1a and ORF2. Therefore, we decided to produce two smaller antigens for each of these latter ORFs instead. ORF1a-p20 and -p26 were designed on the basis of two known products generated after proteolysis of the nsp1a precursor protein in human astroviruses (Geigenmuller et al., 2002). ORF2-con and -var correspond to the conserved and variable regions of Vp90, respectively (Bass and Qiu, 2000; Wang et al., 2001) (Fig. 1).

2.2. RNA extraction, amplification, and cloning

RNA was extracted with TRIzol Reagent (Life Technologies) from frozen brain tissue of animal 45664, the BoAstV-CH13/NeuroS1 index case described in the study of Bouzalas et al. (Bouzalas et al., 2014). Viral RNA was reverse transcribed to cDNA (primer 5′-CTCGGCGTGGCCTCGG-3′) with ThermoScrip RT-PCR System (Life Technologies), which was then amplified by PCR with Pfu DNA Polymerase (Promega) using the following thermal cycling conditions: 95 °C for 2 min, 10 cycles at 95 °C for 30 s, 55 °C for 30 s, 72 °C for 90 s, 25 cycles at 95 °C for 30 s, 60 °C for 30 s, 72 °C for 1 min + 10 s per cycle and 72 °C for 7 min. The primers included restriction enzyme recognition sites that allowed directional cloning into the expression vector (Supplementary material S1). Each amplicon was first cloned into TOPO TA vector (Life Technologies) and transformed into One Shot TOP10 Chemically Competent E. coli (Thermo Fisher Scientific). The insert sequences were verified by Sanger sequencing and subcloned into the expression vector pETHis-1 (Schaller et al., 1999), which encodes for 6× and 10× histidine tags 5′ and 3′ to the insert, respectively. The resulting constructs were finally transformed into BL21 (DE3) Competent Cells C2527 (New England Biolabs).

2.3. Western immunoblot

Expression of each recombinant protein was checked by Western blot, which also allowed the optimization of bacterial growth and expression conditions. Briefly, samples were diluted 1:2 in Laemmli buffer and boiled at 95 °C for 5–10 min. Electrophoresis of the samples was carried out in hand-casted 10% acrylamide Tris-glycine gels and transfer was done to nitrocellulose membranes. After blocking in 5% skim-milk for 1 h in PBS-Tween, membranes were incubated with Mouse Anti Histidine tag, clone AD1.1.10 (AbD Serotec) antibodies, diluted 1:1000 in 5% skim-milk in PBS-Tween for 1 h and, following washing, with Polyclonal Rabbit Anti-Mouse Immunoglobulins/HRP (Dako), diluted 1:9000, for 45 min. Visualization of protein bands was achieved using 1-Step Ultra TMB-Blotting Solution (Thermo Fisher Scientific).

2.4. Recombinant protein expression and purification

Six hundred ml Luria-Bertani medium containing 100 μg/ml ampicillin were inoculated with 25 ml overnight culture of transformed BL21 cells and incubated at 37 °C on a horizontal shaker until reaching an OD_{600} of 0.6–0.8. Expression of recombinant protein was induced by addition of isopropyl-β-D-thiogalactopyranoside (IPTG) to a final concentration of 0.5 mM, the culture being then incubated for 2 h more. The culture volume was divided in three, then bacteria were harvested by centrifugation at $4000 \times g$ for 15 min at 4 °C, and the resulting pellets were stored frozen for at least 30 min. Purification conditions were optimized for each of the recombinant proteins (Supplementary material S2). Lysis of bacteria was performed in 5 ml lysis buffer for 30 min at room temperature, either containing 1 mg/l Lysozyme from chicken egg white (Sigma Aldrich) or 6 M urea. The samples were then sonicated for 4 min in iced water with a Branson sonifier 250 device (Emerson Industrial Automation), using the following parameters: duty cycle 50%, output control 1. The lysates were incubated at 4 °C overnight under gentle agitation, and then cleared by centrifugation for 30 min at $12,000 \times g$ and 4 °C. Afterwards, each recombinant His-tagged protein was immobilized on a HisTrap HP column (GE Healthcare) using an ÄKTAprime plus device (GE Healthcare) as follows: first, the column was washed with 10 ml binding/washing buffer, then the lysate was injected in a 5 ml fraction. After intensive washing with 15 ml binding/washing buffer, the protein was collected in 4 fractions of 1 ml (E1-E4) through step elution using a PBS buffer containing 500 mM imidazole. Eluted fractions were analyzed for protein content and purity by SDS-PAGE and Western blot. Imidazole was removed from the eluted fraction containing the highest quantity of protein by dialysis against in PBS with 1 M urea. Finally, the protein concentration was controlled using a NanoDrop 1000 Spectrophotometer (Thermo Fisher Scientific).

2.5. Rabbit immunization

Immunization and blood sample collection was conducted at Davids Biotechnologie (Regensburg, Germany). Two rabbits per antigen were injected s.c., one with 200–600 μg of protein in solution (SuperFast Antiserum protocol) and the other with 50–200 μg of antigen contained in SDS-PAGE gel pieces (LowDose Antiserum protocol). Pre- and post-immunization sera were collected (1.5 ml and 90 ml, respectively) and 45 ml of each post-immunization serum was affinity-purified. At our institute, all samples were tested for their specific reactivity by Western blotting using the corresponding recombinant proteins.
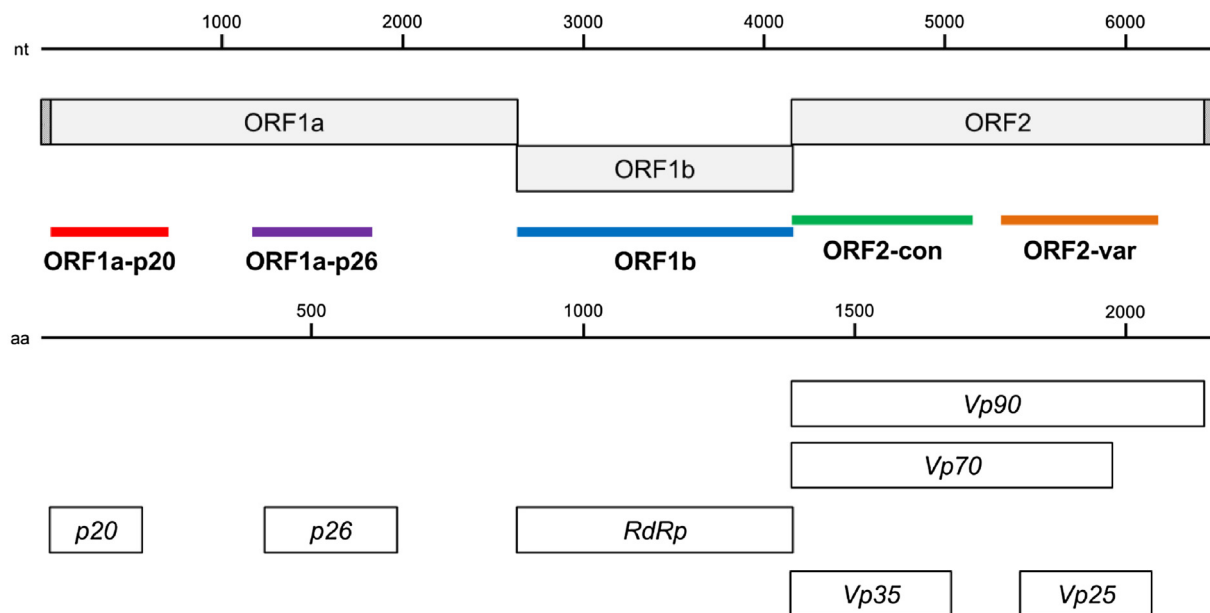
Fig. 1. Relation of recombinant antigens to the BoAstV-CH13/NeuroS1 genome and putative viral proteins. Recombinant antigens are depicted in bold and coding regions are indicated by colors. The slight divergence between antigens ORF1a-p20, respectively ORF1a-p26 and protein products p20, respectively p26 is due to the primer designing step for amplification of viral cDNA. ORF1a, ORF1b, ORF2: characteristic open reading frames of the family *Astroviridae*; in italics: putative protein products of the family *Astroviridae*; hatched genome regions: untranslated regions (UTR); nt: nucleotide; aa: amino acid; RdRp: RNA-dependent RNA polymerase.

2.6. Immunohistochemistry − pre-assessment

After a first screening with 3 different antigen retrieval methods (microwave heating in citrate buffer at pH 6 and pH 9, proteinase K treatment) and dilutions (1:20, 1:50, 1:100), several parameters were evaluated in order to determine the best performing IHC protocol: antigen retrieval method (microwave heating in citrate buffer at pH 6 and pH 9, microwave heating in urea buffer, proteinase K treatment, trypsin treatment, autoclaving in citrate buffer at pH6, no treatment), dilution (1:10, 1:25, 1:50, 1:100, 1:250, 1:500, 1:1000) and incubation time (1 h at 37 °C, overnight at 4 °C) of the primary antibody. Each method was tested on a positive (index case 45664) and negative control (animal 49455, tested negative for BoAstV-CH13/NeuroS1 by RT-PCR and ISH) sample, and the resulting staining assessed microscopically.

2.7. ORF2-con immunohistochemistry

Pre-assessment results led to the establishment of the final IHC protocol with ORF2-con hyperimmune serum. FFPE brain tissue was cut to 4 μm thick sections. After deparaffinization and dehydration of tissue sections, endogenous peroxidase activity was blocked in a solution of 3% H_2O_2 in methanol for 15 min. Antigen retrieval was performed by microwave heating (20 min at 95 °C) in a Microwave Tissue Processor (EBSciences) in Target Retrieval solution, pH 9 (Dako). Subsequently, tissue slides were blocked for 15 min in 10% normal goat serum in PBS-T solution, which was followed by incubation with affinity-purified rabbit hyperimmunsera, diluted 1:100 in PBS-Tween, overnight at 4 °C. Antibody detection was done with Dako REAL Detection System following the manufacturer's instructions and tissue slides were finally counterstained with Mayer's hemalum solution (Merck Millipore).

2.8. Immunohistochemistry − validation procedure

The ORF2-con protocol was further validated using three groups of samples that were available from the archive of the Division of Neurological Sciences, Vetsuisse Faculty, University of Bern (Bern,

Switzerland): (i) 30 tissue samples originating from 9 BoAstV-CH13/NeuroS1 positive animals (either in NGS or RT-PCR), (ii) 30 tissue samples from 8 cattle with viral encephalitis of unknown etiology, which were negative for BoAstV (in NGS, RT-PCR or ISH assays) and (iii) 30 controls, apparently healthy slaughtered, without histopathological brain lesions and that were tested negatively in RT-PCR. Animals of the two first groups presented neurological symptoms and were histologically diagnosed with ESBE. The protocol was also tested with a brain sample of animal 42535, which was found to be positive for BoAstV-CH15 (Seuberlich et al., 2016).

We were also interested to compare the staining obtained in IHC to that in ISH. To this end, we applied a previously described ISH protocol (Bouzalas et al., 2014). Both digoxigenin (DIG)-labeled antisense RNA probes A and B were used.

2.9. Immunofluorescence (IF)

The protocol for IF was the same as for IHC, until and including the incubation step with the primary antibody. Then, after washing 3×5 min with PBS-T, the slides were incubated with Alexa Fluor 555 goat anti-rabbit antibodies (Abcam) diluted 1:100 in PBS-Tween for 1–2 h at room temperature and in the dark. DAPI BioChemica (AppliChem) was then added in a 1:10,000 dilution for 30 min. Ultimately, the slides were washed 3×5 min with PBS-T and 1×5 min with distilled water, and mounted with Glycergel (Dako).

3. Results

3.1. Cloning, recombinant protein expression and purification

All five target sequences were successfully cloned into the expression vector pETHis-1 and recombinant proteins were produced by BL21 E. coli, as proteins of the expected molecular masses could be seen in Western blot with antibodies targeting the histidine tags (Fig. 2A). However, expression levels varied considerably and for two proteins (ORF1a-p20 and ORF1a-p26) strong denaturing conditions were required for protein extraction and
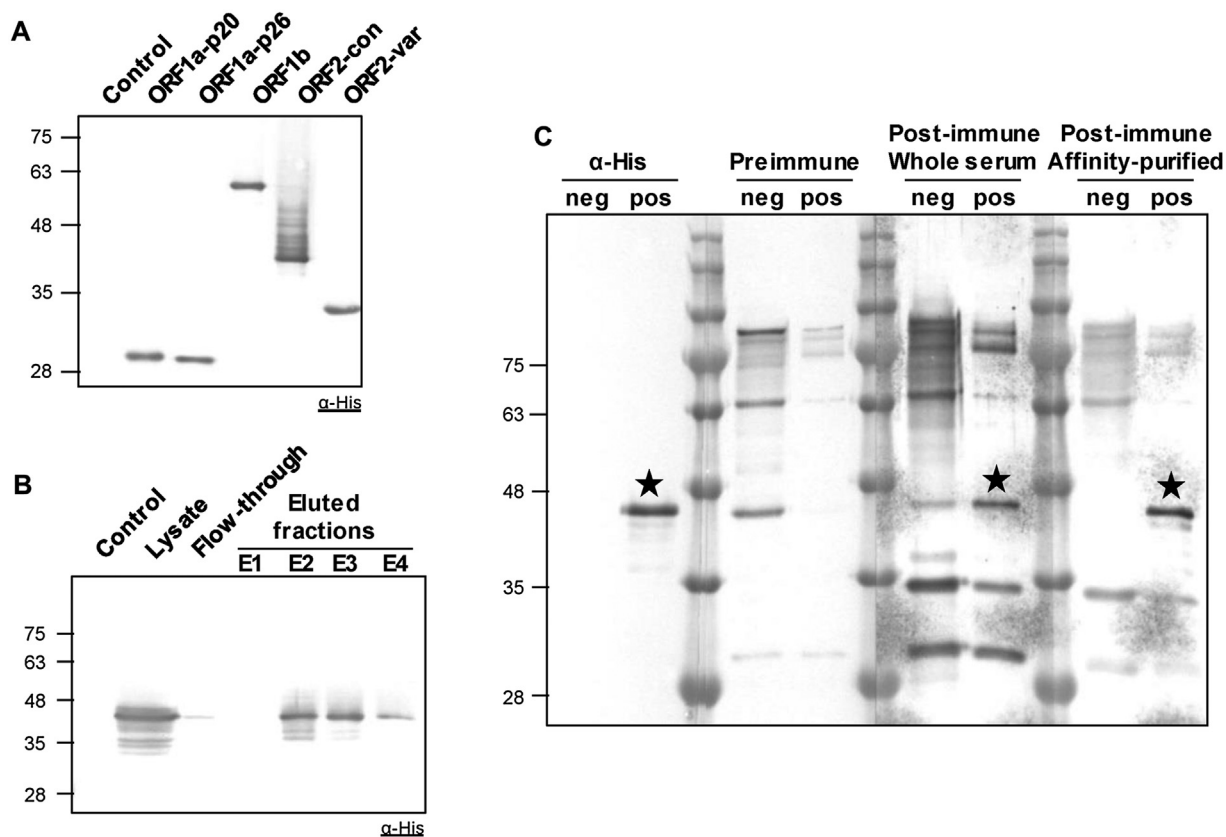
Fig. 2. Detection of recombinant antigens using Western blotting methods. (A) Detection of all five recombinant antigens obtained 2 h after induction of protein expression, using anti-His antibodies. Expected molecular weights (kDa), calculated with the ExPASy ProtParam tool (http://web.expasy.org/protparam): ORF1a-p20: 29.8; ORF1a-p26: 28.9; ORF1b: 63.9; ORF2 con: 41.7; ORF2-var: 36.9. (B) Fractions obtained during protein purification of antigen ORF2-con. Controls in panels A and B: BL21 cells with empty pETHis vector. (C) Testing of the hyperimmune serum raised against ORF2-con on fraction E2 obtained during purification of ORF2-con and a negative control, and comparison with protein staining performed with anti-His monoclonal antibodies and preimmune serum. The band visible at the approximate molecular weight of ORF2-con in the control is most likely due to E. coli-directed antibodies, against which rabbits naturally build an immune response, as this band disappears after affinity-purification of the serum. neg: negative control (fraction E2 obtained during purification of ORF2-var); pos: fraction E2 obtained after purification of ORF2-con; Stars: protein band corresponding to ORF2-con. Molecular mass markers are indicated in kDa on the left.

purification. After metal-chelate affinity purification, the fractions containing the most protein of interest were E2 and E3 for all recombinant proteins (as exemplified for the ORF2-con protein in Fig. 2B). A minimum protein quantity of 0.2 mg (minimal concentration: 0.3 mg/ml) in solution after dialysis or 50 μg in gel pieces in total was achieved for all proteins, which was considered as sufficient for rabbit immunization.

3.2. Rabbit immunization

All five hyperimmune sera presented an ELISA titer of 1:30,000 and at least 0.7 mg/ml IgG in the affinity-purified fraction, according to the data provided by the commercial immunization service. In our laboratory, the sera raised against ORF1a-p26, ORF1b, ORF2-con and ORF2-var, but not the one against ORF1a-p20, clearly detected the corresponding recombinant antigen when tested for their immunoreactivity by Western blotting. Yet, reactivity against different putative bacterial proteins could be seen when testing both pre- and hyperimmune sera. The best result was systematically achieved with the affinity-purified fraction of each serum, when compared to the whole serum. The Western blot data for the serum against ORF2-con are shown as an example in Fig. 2C.

3.3. Immunohistochemistry

Affinity-purified hyperimmune sera were tested on FFPE brain tissue sections of a BoAstV-CH13/NeuroS1 positive animal and of a negative one. Sera raised against ORF1a-p20, ORF1a-p26, ORF1b and ORF2-var showed some immunoreactivity on positive sections, but diffuse background staining on negative sections as well, even under optimized conditions (Supplementary material S3). By contrast, when using the serum directed against the ORF2-con antigen, a high number of neurons in the positive sample revealed a strong diffuse and granular cytoplasmic reactivity that extended into their processes (Fig. 3A), which was absent in the negative control tissue (Fig. 3B and C). Based on these results, the IHC protocol using the serum against ORF2-con was selected for further validation.

3.4. Validation of the ORF2-con IHC procedure

Out of 9 BoAstV-CH13/NeuroS1 positive cattle, 8 showed positive immunolabeling in at least one brain region tested and were therefore classified as positive in the ORF2-con IHC. Labeling was absent in the BoAstV-CH13/NeuroS1 negative ESBE cases, as well as in the negative control animals, and consequently these cases scored IHC negative (Table 1). These results indicate a good diagnostic sensitivity (8/9) and a very good diagnostic specificity (38/38) of the ORF2-con IHC.

The amount of immunolabeled cells was variable between brain regions as well as between animals (Table 2). For animal 43484, only one region out of four was positive and the labeling was discrete, as only a few small cells and what appeared as cellular processes were stained. In the remaining IHC positive cases, reactivity was observed in all brain regions (Table 2).
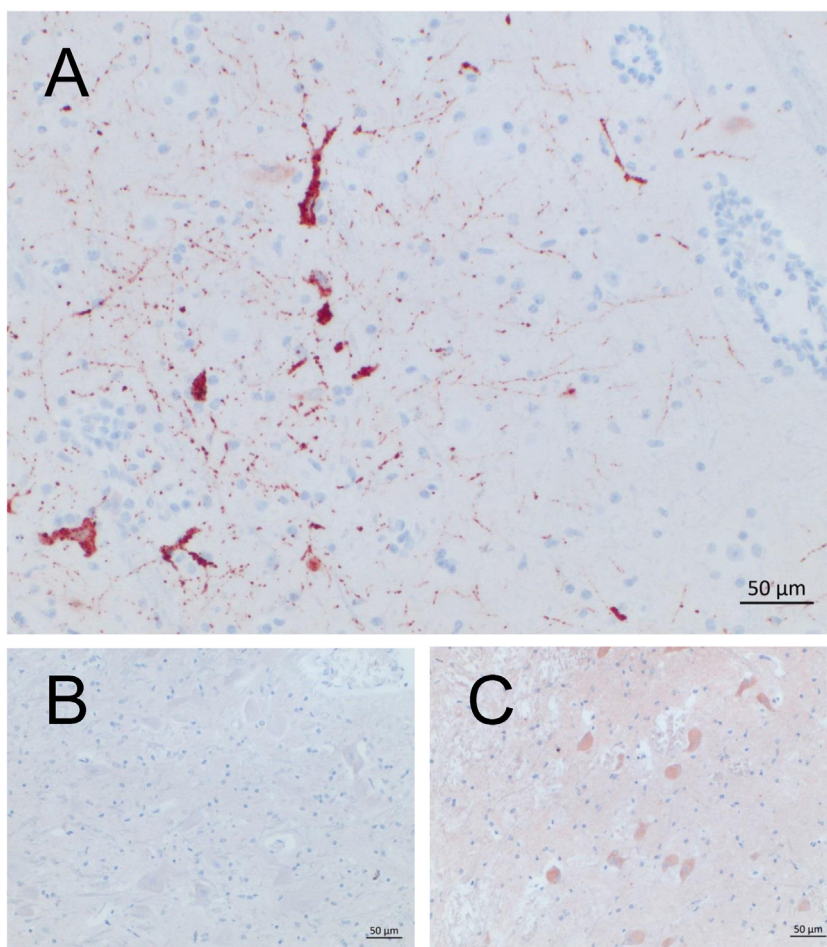
Fig. 3. Immunohistochemical detection of BoAstV-CH13/NeuroS1 in bovine brain tissue using hyperimmune antiserum against ORF2-con. (A) BoAstV-CH13/NeuroS1 positive case. Positively stained cells are strongly labeled, with the presence of granular material. Note perivascular cuffing on the right and gliosis on the left of the picture, which are hallmarks of non-suppurative encephalitis. (B) Negative, healthy control animal. (C) Negative, healthy control animal. Background staining is higher, with some cells appearing diffusely reddish; however, there is none of the granular dark red labeling as seen in positive cases. (For interpretation of the references to colour in this figure legend, the reader is referred to the web version of this article.)

Table 1
Results of BoAstV-CH13/NeuroS1 detection by immunohistochemistry (IHC) in all three animal groups tested for the validation of the protocol. ESBE: European sporadic bovine encephalitis; +: positive; −: negative;.

IHC	ESBEBoAstV+	ESBEBoAstV-	Negativecontrols
+	8	0	0
−	1	8	30
Total	9	8	30

In order to compare the performance of the ORF2-con IHC with ISH, serial sections of different brain regions of the BoAstV-CH13/NeuroS1 index case 45664 were tested by ISH and IHC. The dissemination of positively stained cells in IHC was very similar in all brain regions compared to ISH (Fig. 4A and B). Nonetheless, in IHC, cell staining was more easily recognizable and more uniform, tissue architecture was better conserved and there was in general much less background staining compared to ISH. The hyperimmune serum against ORF2-con apparently does not recognize the BoAstV-CH15 virus, as labeling was absent in animal 42535.

3.5. Immunofluorescence

We were interested in whether the hyperimmune serum against ORF2-con is also suitable for the detection of viral antigens by immunofluorescence (IF) in FFPE tissues. Although this approach was not fully validated, in the index case 45664, the distribution of positively stained cells was comparable to that in IHC and ISH (Fig. 4A–C). Staining appeared as granula-like material spread over the entire cytoplasm of affected cells, including fine processes, and apart from the nucleus that was clearly visible through DAPI staining. Based on morphological criteria only, these cells were classified as neurons (Fig. 5).

4. Discussion

Considering general knowledge on structural and nonstructural proteins of *Astroviridae*, five different antigens of the neurotropic astrovirus BoAstV-CH13/NeuroS1 were expressed in E.coli and purified by metal-chelate affinity chromatography. Purified proteins were then used for the production of hyperimmune sera in rabbits. The polyclonal antibodies obtained were finally employed for the development of a reliable detection method for that virus in FFPE brain tissues.

Although four out of the five polyclonal antibodies showed specific reactivity in Western immunoblot against the corresponding antigen used for immunization, only the hyperimmune serum against ORF2-con gave a good signal-to-noise ratio in IHC. A first explanation to this may be linked to insufficient antigen retrieval in FFPE tissues, as most hyperimmune sera still showed specific reactivity against their antigen in Western blotting assays. On the
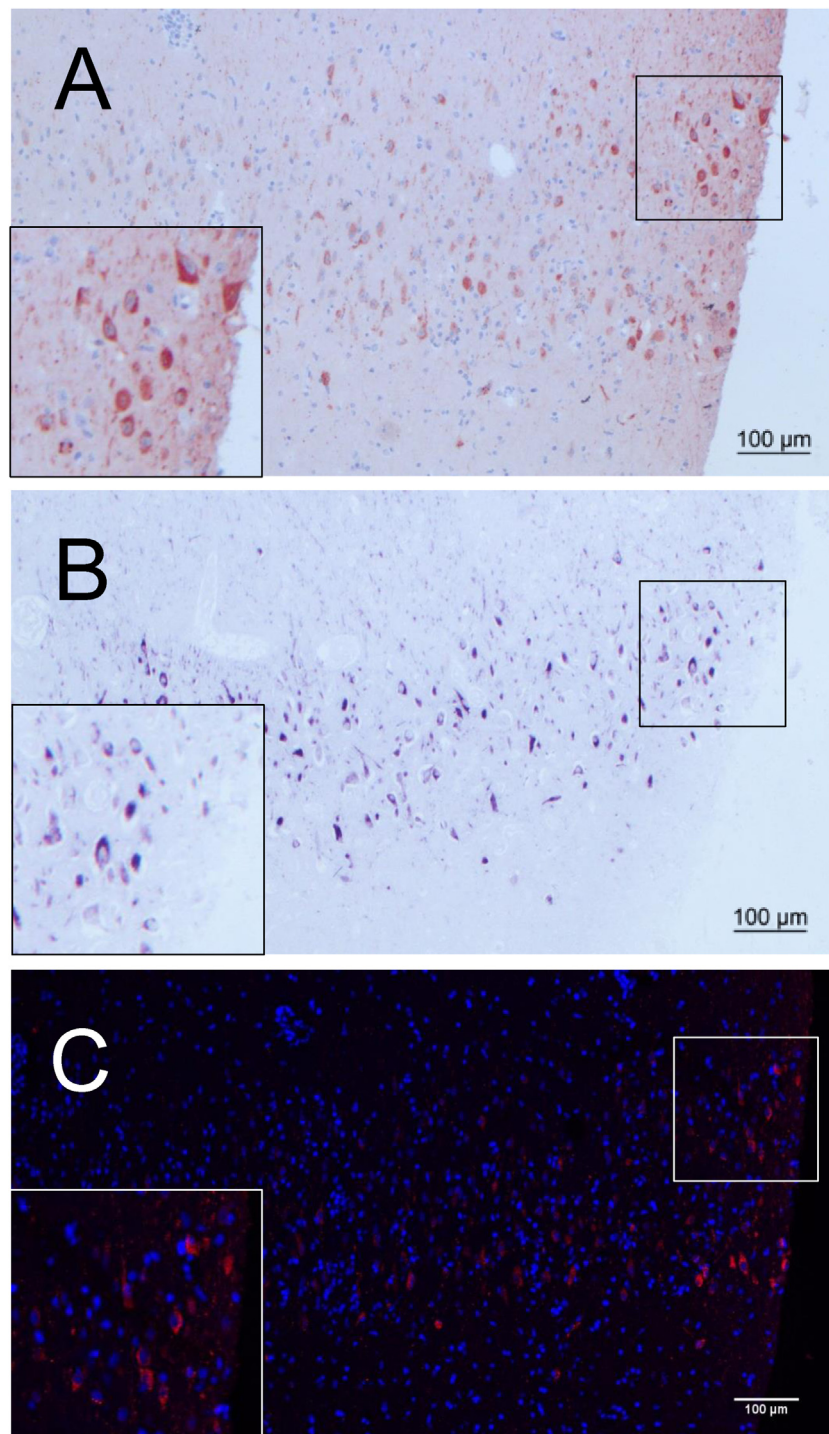
Fig. 4. Comparison of BoAstV-CH13/NeuroS1 staining using different methods, on serial tissue sections of a part of the hippocampus of index case 45664. (A) Immuno-histochemistry. (B) *In situ* hybridization with probe B. (C) Immunofluorescence; red: ORF2-con; blue: DAPI. The inset on the lower corner of each picture shows a higher magnification of the respective zone highlighted on the right.

other hand, the good reactivity of the hyperimmune serum against ORF2-con in IHC could be due to higher expression levels of structural viral proteins in infected tissues compared to nonstructural proteins, a fact that is well known for many viruses. The hyperimmune serum against ORF1a-p20 was the only one that lacked reactivity against the corresponding recombinant protein in Western blot and against BoAstV-CH13/NeuroS1 antigens in IHC, which may result from low immunogenicity of the recombinant protein or from the antibodies being directed primarily against discontin-

uous epitopes, which were not preserved under formalin fixation and denaturing conditions in Western immunoblot, respectively. In spite of this, the hyperimmune sera obtained, including those that did not perform in IHC in a satisfactory manner, will be tested with different immunological assays, such as immunoprecipitation, antigen ELISA or in order to study the virus biology, for instance in cell culture models. Conversely, the antigens produced will be assed for the development of ELISA techniques to detect virus spe-

Table 2
Detailed results of BoAstV-CH13/NeuroS1 detection by immunohistochemistry (IHC) in different tissue samples of animals with a known positive status for the virus. NGS: next-generation sequencing; ISH: *in situ* hybridization; +: positive; −: negative; nd: not done; numbers in brackets: semi quantitative evaluation of positivity in IHC.

| Case no	NGS	RT-PCR	Region	ISH	IHC
23871	+	+	brainstem	+	+ (3)
			midbrain	+	+ (3)
23985	+	+	cerebellum, brainstem	+	+ (3)
			cerebellum, brainstem	−	+ (2)
			cerebrum cortex	+	+ (3)
26730	+	nd	cerebellum, brainstem	+	+ (2)
			cerebrum (hippocampus)	+	+ (3)
			cerebellum, brainstem	+	+ (1)
26875	+	+	cerebrum cortex	+	+ (1)
			cerebellum, brainstem	+	+ (1)
			cerebellum, brainstem	+	+ (3)
			brainstem	+	+ (3)
36716	+	nd	brainstem	+	+ (1)
			cerebellum, brainstem	+	+ (2)
			cerebellum	−	+ (1)
			cerebrum (hippocampus)	+	+ (2)
43484	nd	+	brainstem	−	−
			brainstem	−	−
			cerebrum (thalamus)	+	+ (1)
			cerebrum cortex	−	−
43660	+	nd	cerebellum, brainstem	+	+ (1)
			cerebellum, brainstem	+	+ (1)
			cerebrum (hippocampus)	−	+ (3)
			cerebrum cortex	−	+ (1)
43661	+	nd	brainstem (obex)	−	−
			cerebellum, brainstem	−	−
50773	nd	+	brainstem	+	+ (2)
			midbrain	+	+ (3)
			cerebrum (hippocampus)	+	+ (3)
			cerebrum cortex	+	+ (3)
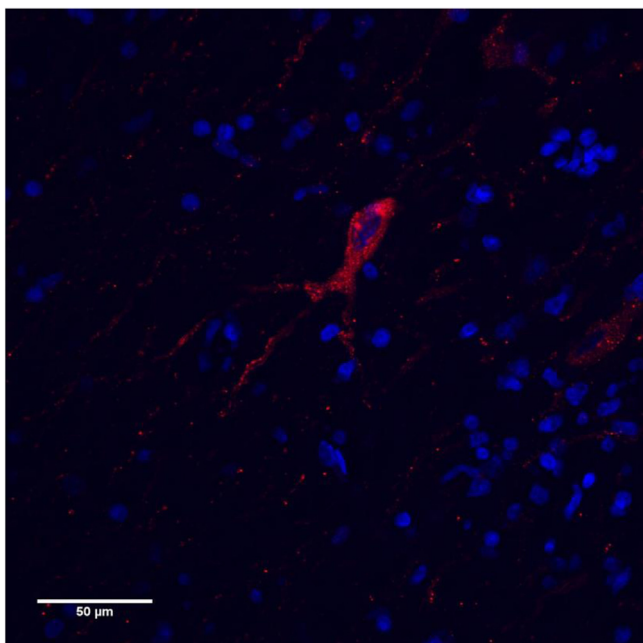
Fig. 5. High magnification of a cell stained with hyperimmune serum against ORF2-con in immunofluorescence.

cific antibodies and to conduct seroprevalence estimations in the cattle population.

The ORF2-con IHC protocol was further validated for the purpose of BoAstV-CH13/NeuroS1 detection in FFPE tissues. None of the virus negative animals was positive in the ORF2-con IHC. Inversely, all but one virus positive animal were positive in the ORF2-con IHC. In animal 43661 BoAstV CH13/NeuroS1 was detected by NGS but neither by ISH, nor by IHC. This finding was unexpected, since

these last two methods are usually able to detect single infected cells in larger sections of brain tissue, whereas virus detection by NGS is done in relatively small tissue samples and may be technically challenging. We reported previously the full-length sequence of the virus isolate in this animal and it was found to be genetically very similar to the reference strain (Bouzalas et al., 2016). This argues against this particular isolate being a divergent type of astrovirus. However, it was also not fully identical to other isolates sequenced in our previous studies, thus laboratory contamination of this brain sample appears unlikely. On the other hand, we cannot exclude an environmental contamination during sampling. It is worth mentioning that the read-coverage and read–depth in NGS were low for this particular isolate, a fact that implies a low viral load. Therefore, these divergent test results may reflect an uneven virus distribution in the brain tissue, rather than differences in the detection limit of NGS compared to that of IHC and ISH.

We analyzed sections of the same FFPE blocks of all virus positive animals by IHC and ISH, which allowed a good comparison of the sensitivity of both techniques. While all blocks that tested positive in ISH were also positive in IHC, this was not the case in the opposite situation, namely for three animals, IHC detected BoAstV-CH13/NeuroS1 in more brain regions than ISH (Table 2). This argues for a slightly higher sensitivity of the ORF2-con IHC compared to the detection of viral RNA by ISH. Moreover, the IHC protocol is much faster, easier to perform and preserves the tissue architecture better than ISH. In this regard, the new IHC protocol is superior to ISH and will replace it in routine testing for BoAstVCH13/NeuroS1 in FFPE brain tissues in our laboratory.

In addition to a pure diagnostic application of the ORF2-con hyperimmune serum, double-staining IF against ORF2-con and specific cell markers would allow to further investigate which neuronal and potentially extraneuronal cell types are infected by BoAstVCH13/NeuroS1.

This novel IHC tool allows a broader testing of brain tissue of cattle and other species affected with non-suppurative encephalitis of

unknown etiology, in retrospective as well as prospective studies. In that sense, it would be interesting to investigate if the protocol also works for neurotropic bovine astroviruses originating from other geographical areas. We provided first evidence that BoAstV-CH15 (which is phylogenetically distinct from the CH13/NeuroS1 species) is not detected by the ORF2-con IHC, and the same may also count for BoAstV-BH89/14, which has been reported recently in Germany (Schlottau et al., 2016). IHC techniques for these viruses will likely require the development of adapted recombinant antigens and the production of dedicated antibodies.

Many aspects on the relationship of neurotropic astroviruses and encephalitis remain unclear. The role of co-infections or immunodeficiency in disease (as it seems to be the case in humans) is unknown, pathogenesis and transmission are not elucidated and, importantly, nothing is known about a possible zoonotic potential of these viruses, all of which being elements prompting further research on the topic. With the present study, we have extended the spectrum of available diagnostic tools, which is a prerequisite for these research activities.

Conflicts of interest

The authors declare no conflict of interest.

Acknowledgements

Appendix A. Supplementary data

Supplementary data associated with this article can be found, in the online version, at http://dx.doi.org/10.1016/j.jviromet.2016.10.013.

References

Alfred, N., Liu, H., Li, M.L., Hong, S.F., Tang, H.B., Wei, Z.Z., Chen, Y., Li, F.K., Zhong, Y.Z., Huang, W.J., 2015. Molecular epidemiology and phylogenetic analysis of diverse bovine astroviruses associated with diarrhea in cattle and water buffalo calves in China. J. Vet. Med. Sci. 77, 643–651.

Appleton, H., Higgins, P.G., 1975. Letter: viruses and gastroenteritis in infants. Lancet (London, England) 1, 1297.

Bass, D.M., Qiu, S., 2000. Proteolytic processing of the astrovirus capsid. J. Virol. 74, 1810–1814.

Blomstrom, A.L., Widen, F., Hammer, A.S., Belak, S., Berg, M., 2010. Detection of a novel astrovirus in brain tissue of mink suffering from shaking mink syndrome by use of viral metagenomics. J. Clin. Microbiol. 48, 4392–4396.

Bouzalas, I.G., Wuthrich, D., Walland, J., Drogemuller, C., Zurbriggen, A., Vandevelde, M., Oevermann, A., Bruggmann, R., Seuberlich, T., 2014. Neurotropic astrovirus in cattle with nonsuppurative encephalitis in Europe. J. Clin. Microbiol. 52, 3318–3324.

Bouzalas, I.G., Wuthrich, D., Selimovic-Hamza, S., Drogemuller, C., Bruggmann, R., Seuberlich, T., 2016. Full-genome based molecular characterization of encephalitis-associated bovine astroviruses. Infect. Genet. Evol. 44, 162–168.

Brown, J.R., Morfopoulou, S., Hubb, J., Emmett, W.A., Ip, W., Shah, D., Brooks, T., Paine, S.M., Anderson, G., Virasami, A., Tong, C.Y., Clark, D.A., Plagnol, V., Jacques, T.S., Qasim, W., Hubank, M., Breuer, J., 2015. Astrovirus VA1/HMO-C: an increasingly recognized neurotropic pathogen in immunocompromised patients. Clin. Infect. Dis. 60, 881–888.

Caul, E.O., Appleton, H., 1982. The electron microscopical and physical characteristics of small round human fecal viruses: an interim scheme for classification. J. Med. Virol. 9, 257–265.

Cordey, S., Vu, D.L., Schibler, M., L'Huillier, A.G., Brito, F., Docquier, M., Posfay-Barbe, K.M., Petty, T.J., Turin, L., Zdobnov, E.M., Kaiser, L., 2016. Astrovirus MLB2, a new gastroenteric virus associated with meningitis and disseminated infection. Emerg. Infect. Dis. 22, 846–853.

Fankhauser, R., 1961. Sporadic meningoencephalomyelitis in cattle. Schweiz. Arch. Tierheilkd. 103, 225–235.

Fremond, M.L., Perot, P., Muth, E., Cros, G., Dumarest, M., Mahlaoui, N., Seilhean, D., Desguerre, I., Hebert, C., Corre-Catelin, N., Neven, B., Lecuit, M., Blanche, S., Picard, C., Eloit, M., 2015. Next-generation sequencing for diagnosis and tailored therapy: a case report of astrovirus-associated progressive encephalitis. J. Pediatr. Infect. Dis. Soc. 4, e53–e57.

Geigenmuller, U., Chew, T., Ginzton, N., Matsui, S.M., 2002. Processing of nonstructural protein 1a of human astrovirus. J. Virol. 76, 2003–2008.

Li, L., Diab, S., McGraw, S., Barr, B., Traslavina, R., Higgins, R., Talbot, T., Blanchard, P., Rimoldi, G., Fahsbender, E., Page, B., Phan, T.G., Wang, C., Deng, X., Pesavento, P., Delwart, E., 2013. Divergent astrovirus associated with neurologic disease in cattle. Emerg. Infect. Dis. 19, 1385–1392.

Naccache, S.N., Peggs, K.S., Mattes, F.M., Phadke, R., Garson, J.A., Grant, P., Samayoa, E., Federman, S., Miller, S., Lunn, M.P., Gant, V., Chiu, C.Y., 2015. Diagnosis of neuroinvasive astrovirus infection in an immunocompromised adult with encephalitis by unbiased next-generation sequencing. Clin. Infect. Dis. 60, 919–923.

Quan, P.L., Wagner, T.A., Briese, T., Torgerson, T.R., Hornig, M., Tashmukhamedova, A., Firth, C., Palacios, G., Baisre-De-Leon, A., Paddock, C.D., Hutchison, S.K., Egholm, M., Zaki, S.R., Goldman, J.E., Ochs, H.D., Lipkin, W.I., 2010. Astrovirus encephalitis in boy with X-linked agammaglobulinemia. Emerg. Infect. Dis. 16, 918–925.

Sato, M., Kuroda, M., Kasai, M., Matsui, H., Fukuyama, T., Katano, H., Tanaka-Taya, K., 2016. Acute encephalopathy in an immunocompromised boy with astrovirus-MLB1 infection detected by next generation sequencing. J. Clin. Virol. 78, 66–70.

Saylor, D., Thakur, K., Venkatesan, A., 2015. Acute encephalitis in the immunocompromised individual. Curr. Opin. Infect. Dis. 28, 330–336.

Schaller, A., Kuhn, R., Kuhnert, P., Nicolet, J., Anderson, T.J., MacInnes, J.I., Segers, R.P., Frey, J., 1999. Characterization of apxIVA, a new RTX determinant of Actinobacillus pleuropneumoniae. Microbiology (Reading, England) 145 (Pt 8), 2105–2116.

Schlottau, K., Schulze, C., Bilk, S., Hanke, D., Hoper, D., Beer, M., Hoffmann, B., 2016. Detection of a novel bovine astrovirus in a cow with encephalitis. Transbound. Emerg. Dis. 63, 253–259.

Seuberlich, T., Wuthrich, D., Selimovic-Hamza, S., Drogemuller, C., Oevermann, A., Bruggmann, R., Bouzalas, I., 2016. Identification of a second encephalitis-associated astrovirus in cattle. Emerg. Microbes Infect. 5, e5.

Tse, H., Chan, W.M., Tsoi, H.W., Fan, R.Y., Lau, C.C., Lau, S.K., Woo, P.C., Yuen, K.Y., 2011. Rediscovery and genomic characterization of bovine astroviruses. J. Gen. Virol. 92, 1888–1898.

Wang, Q.H., Kakizawa, J., Wen, L.Y., Shimizu, M., Nishio, O., Fang, Z.Y., Ushijima, H., 2001. Genetic analysis of the capsid region of astroviruses. J. Med. Virol. 64, 245–255.

Woode, G.N., Bridger, J.C., 1978. Isolation of small viruses resembling astroviruses and caliciviruses from acute enteritis of calves. J. Med. Microbiol. 11, 441–452.

Woode, G.N., Pohlenz, J.F., Gourley, N.E., Fagerland, J.A., 1984. Astrovirus and Breda virus infections of dome cell epithelium of bovine ileum. J. Clin. Microbiol. 19, 623–630.

Wunderli, W., Meerbach, A., Gungor, T., Berger, C., Greiner, O., Caduff, R., Trkola, A., Bossart, W., Gerlach, D., Schibler, M., Cordey, S., McKee, T.A., Van Belle, S., Kaiser, L., Tapparel, C., 2011. Astrovirus infection in hospitalized infants with severe combined immunodeficiency after allogeneic hematopoietic stem cell transplantation. PLoS One 6, e27483.